

A Forward-Backward Strategy for Handling Non-linearity in Electrical Impedance Tomography

Martin Huska(✉), Damiana Lazzaro, and Serena Morigi

Department of Mathematics, University of Bologna, Bologna, Italy
{martin.huska,damiana.lazzaro,serena.morigi}@unibo.it

Abstract. Electrical Impedance Tomography (EIT) is known to be a nonlinear and ill-posed inverse problem. Conventional penalty-based regularization methods rely on the linearized model of the nonlinear forward operator. However, the linearized problem is only a rough approximation of the real situation, where the measurements can further contain unavoidable noise. The proposed reconstruction variational framework allows to turn the complete nonlinear ill-posed EIT problem into a sequence of regularized linear least squares optimization problems via a forward-backward splitting strategy, thus converting the ill-posed problem to a well-posed one. The framework can easily integrate suitable penalties to enforce smooth or piecewise-constant conductivity reconstructions depending on prior information. Numerical experiments validate the effectiveness and feasibility of the proposed approach.

Keywords: EIT inverse problem · Forward-backward algorithm · Nonlinear optimization · Regularization

1 Introduction

Electrical impedance tomography (EIT) is the problem of determining the electrical conductivity distribution of an unknown medium by making voltage and current measurements at the boundary of the object. As a radiation-free non-invasive monitoring tool, EIT has attracted much attention in the last two decades in a variety of biomedical applications. EIT is a typical ill-posed inverse problem, in the sense that the solution to the inverse problem can fail to exist or be extremely sensitive to small errors in the observations [4]. Since in practice all measurements in EIT experimental setup incorporate noise, a naive solution of this inverse problem with noisy data is typically a meaningless solution. Moreover, differently from the well-assessed tomographic imaging modalities, e.g., computed tomography (CT) and magnetic resonance imaging (MRI), the image reconstruction problem of EIT is characterized by a highly nonlinear forward operator. The forward EIT operator allows calculation of EIT measurement data from a given conductivity distribution.

© Springer Nature Switzerland AG 2021
O. Gervasi et al. (Eds.): ICCSA 2021, LNCS 12951, pp. 635–651, 2021.
https://doi.org/10.1007/978-3-030-86970-0_44

To reduce the ill-posedness, a regularization term is commonly introduced in the mathematical model to use the prior information to constrain the conductivity reconstruction problem. The prior information represents the distribution characteristics of the target conductivity, e.g., smooth, blocky, or sparse, and is modeled by a specially designed regularization term, e.g., Tikhonov, total variation (TV), or ℓ_1-norm [9]. To simplify the computational difficulty of the EIT inverse problem, classical regularization methods rely on the linearized model of the nonlinear forward operator. However, the linearization of the EIT formulation is only a rough approximation of the real measurement system, and this affects the reconstruction results.

We propose a variational framework for EIT reconstructions, which allows to solve the nonlinear ill-posed EIT problem via a forward-backward splitting iterative strategy where a sequence of regularized linear optimization problems are solved, thus turning the ill-posed problem to a sequence of well-posed ones.

The proximal Forward–Backward algorithm is a standard first-order optimization method to minimize a function which is defined as the sum of a differentiable function f and an easily proximable proper lower semicontinuous function g, and it consists in alternating a gradient step on f and a proximal step on g. In the proposed variational framework the proximal step involves a penalty which, according to the a priori knowledge on the conductivity distribution, can be either Tiknonov-like or Total-Variation-like. In the former case we enforce smooth reconstructions, while in the latter we assume piecewise-constant conductivity distribution as the prior information.

The paper is organized as follows. The remaining of this section is devoted to a brief overview on variational approaches to the EIT problem. In Sect. 2 notations and the inverse EIT formulation are introduced. Section 3 formulates the regularized Gauss-Newton method for the EIT problem. The proposed variational approach and the forward-backward iterative strategy are described in Sect. 4. Numerical experiments validate the effectiveness and feasibility of the proposed approach in Sect. 5. Conclusions are drawn in Sect. 6.

1.1 Related Works

Variational approaches to the solution of the EIT problem are currently the most successful and widely used both for linearized and non-linearized EIT reconstruction methods. A well-known variational formulation for linearized EIT problems relies on a least squares formulation with Tikhonov regularizer to favour smooth conductivity reconstructions [12]. Generalized Tikhonov approaches allow for a more general smoothing penalty term, which includes approximations of differential operators or structural priors [17]. To promote the reconstruction of piece-wise constant conductivity regions, many variational approaches included another common regularizer which relies on the ℓ_1 norm since it maintains the discontinuities in the reconstructed profiles. This regularization method is generally referred to as Total Variation (TV) [3]. This feature makes it particularly suited for medical and industrial applications (e.g. definition of inter-organ and

inter-phase boundaries). However, the use of the TV functional for regularization leads to the minimization of a non-differentiable objective function in the inverse formulation.

The numerical solution of the optimization problems derived from the linear EIT variational approaches with linear regularizers reduces to the use of an efficient solver for linear systems, while the presence of a non-differentiable regularizer, such as the TV one, leads to more sophisticated optimization strategies such as Alternating Directions Method of Multipliers [9], or Primal Dual - Interior Point Method (PD-IPM) [3].

For what concerns the optimization methods for the nonlinear EIT inverse formulations, the literature is based on the Regularized Gauss-Newton (RGN) method. The Newton One-Step Algorithm (NOSER [6]), which performs only the first step of the Gauss-Newton's method with linear regularizer, represents a significant milestone in the investigation of EIT solvers. In [2] the GN method is enriched with an Iterative Reweighted strategy to deal with the non-differentiability of the TV regularizer. A relaxed inexact proximal Gauss–Newton method is proposed in [11] which deals with non-smooth TV regularization to better track the sharp edges in the conductivity.

We propose a reconstruction variational framework for the solution of the non-linear least squares EIT inverse problem which allows to include both linear and non-linear regularization and leads to the solution of a sequence of simple regularized linear least squares optimization problems via a forward-backward splitting strategy, thus converting the ill-posed problem into a well-posed one.

2 Inverse EIT Formulation

In inverse EIT, small alternating currents are applied to conducting surface electrodes attached at the boundary of the object Ω. The measured voltages V_m on the electrodes are used to reconstruct electrical conductivity distribution σ of the internal part of the object.

In the corresponding forward EIT problem one wants to find the electric potential u in the interior of the object Ω and at the electrodes, given some applied current and inner conductivity σ. Following the accurate Complete Electrode Model (CEM), introduced in [5], the forward EIT problem can be formulated as follows:

$$\begin{cases} \nabla \cdot (\sigma(x)\nabla u(x)) = 0 \text{ in} & \Omega, \\ u + z_l \sigma \frac{\partial u}{\partial n} = V_l & \text{on} \quad E_l,\ l = 1, .., L, \\ \int_{E_l} \sigma \frac{\partial u}{\partial n}\, \mathrm{d}s = I_l & \text{on} \quad \Gamma, \\ \sigma \frac{\partial u}{\partial n} = 0 & \text{on} \quad \tilde{\Gamma}, \end{cases} \tag{1}$$

where Γ ($\tilde{\Gamma}$) is the boundary $\partial\Omega$ with (without) electrodes, V_l is the unknown voltage to be measured by l-th electrode E_l when the currents I_l are applied, z_l

are the contact impedances. The solution of forward EIT problem amounts to solving the boundary problem (1).

The *Forward Operator* $\tilde{F}$, which operates between the Hilbert spaces X and Y, maps the conductivity σ to the solution of the forward problem:

$$\begin{aligned} \tilde{F}\colon \mathfrak{S} \subset X &\to Y \\ \sigma &\mapsto (u, V) \end{aligned} \tag{2}$$

where $\mathfrak{S} = \{\sigma \in L^\infty(\Omega) \mid \sigma \nabla u = 0\}$, denotes the domain of definition of $\tilde{F}$.

Proposition 1: The operator $\tilde{F}$ that maps $\sigma \in \mathfrak{S}$ to the solution of the Forward Problem with current vector I is Fréchet differentiable, meaning that

$$\lim_{\|\delta\sigma\|_\infty \to 0} \frac{\|\tilde{F}(\sigma + \delta\sigma) - \tilde{F}(\sigma) - \tilde{F}'(\sigma)\delta\sigma\|_Y}{\|\delta\sigma\|_\infty} = 0. \tag{3}$$

The proof of Proposition (1) is provided in [14], where it is also proved that $\tilde{F}'$ is Lipschitz continuous.

From now on we restrict the conductivities σ to a finite dimensional space of piecewise polynomials. We consider the object domain Ω discretized into n_T subdomains $\{\tau_j\}_{j=1}^{n_T}$ and σ constant over each of them. Given a Finite Elements Model (FEM) of an EIT medium, we calculate the vector of voltages, V_m, for each FEM degree of freedom. For a given stimulation pattern a vector of n_M measurements is acquired, obtained by injecting current through an electrodes pair and then measuring the corresponding voltage V_m induced on another pair of electrodes. Then $F : \mathbb{R}^{n_T} \to \mathbb{R}^{n_M}$ represents the discrete version of the Forward Operator (2) as a nonlinear vector map.

Since $\tilde{F}$ is Fréchet differentiable, F' is a matrix, called the Jacobian of F and denoted by J; each element of $J \in \mathbb{R}^{n_M \times n_T}$ is defined as

$$\{J(u_d, u_m)\}_{i,j} = \int_{\tau_j} \nabla u_d \cdot \nabla u_m d\Omega \,, \tag{4}$$

where the row index i corresponds to the ith measurement, associated with the dth driving potential u_d and mth measurement potential u_m, while the column index j corresponds to the subdomain τ_j.

Considering measured data corrupted by additive noise, we can assume the following noisy non-linear observation model

$$V_m = F(\sigma) + \eta, \tag{5}$$

where $V_m \in \mathbb{R}^{n_M}$ represents the vector of all the measured electrode potentials whose dimension n_M depends on the choice of a measurement protocol, and $\eta \in \mathbb{R}^{n_M}$ is a zero-mean Gaussian distributed measurement noise vector.

Assuming the non-linear degradation model (5) and the given measurements V_m, the so called absolute imaging problem aims to estimate the (static) conductivity σ by solving the following **non-linear** least squares problem

$$\sigma^* = \arg\min_{\sigma} f(\sigma), \qquad f(\sigma) = \int_{\Omega} (F(\sigma) - V_m)^2 \, \mathrm{d}\Omega. \tag{EITNL}$$

The underlying optimization problem is hard to solve, as the boundary currents depend non-linearly on the conductivity. This means that the optimization problem is nonconvex.

For the reconstruction of small conductivity changes, conventional approaches rely on the simplest linearized model of the non-linear forward operator F,

$$F(\sigma) \approx F(\sigma_0) + J\delta\sigma = F(\sigma_0) + J(\sigma - \sigma_0), \tag{6}$$

where J represents the Jacobian matrix defined in (4), and calculated at the initial conductivity estimate σ_0. The reconstruction is thus obtained by solving the following **linear** least squares problem

$$\delta\sigma^* = \arg\min_{\delta\sigma} f(\delta\sigma), \qquad f(\delta\sigma) = \int_{\Omega} (J\,\delta\sigma - \delta V_m)^2 \, \mathrm{d}\Omega, \tag{EITL}$$

where $\delta\sigma = \sigma - \sigma_0$ and $\delta V_m = V_m - F(\sigma_0)$.

A benefit of the linear approach is that it leads to computationally fast reconstruction, however, the linearization leads to a very ill-conditioned undetermined linear system to solve, and the solution is only valid for sufficiently small deviations from the conductivity σ_0 at which the Jacobian is initially calculated.

In difference imaging model for EIT, the goal is to reconstruct the change in conductivity between two states measured at different times. The conductivity reconstruction in difference imaging is conventionally carried out using a linear approach as in (EITL), based on the difference of the two data sets and the linearization of the forward model (6). In absolute imaging mode the conductivity distribution is reconstructed even in case only the data after the conductivity change is available (background material conductivity σ_0 is not known). However, absolute reconstructions seem to be less robust with respect to modelling errors caused by inaccurately known boundary shape and electrode positions. To account for modelling errors and, at the same time, to avoid the linear approximation of the forward model, one approach is to compute absolute reconstructions of the conductivities σ_0 and σ based on each of the data sets separately, and then to subtract σ_0 from σ to obtain $\delta\sigma$.

The conductivity change $\delta\sigma$ is reconstructed clearly better by the nonlinear observation model over the conventional approach of using difference imaging with a globally linearized observation model [13].

This motivated us to propose an efficient solution to the non-linear optimization problem (EITNL).

3 Regularized Gauss-Newton for EITNL

The Gauss-Newton method is the most commonly used one for minimizing nonlinear least squares (NLLS) problems such as the EITNL and performs a line search strategy with a specific choice of a descent direction. It simplifies the Newton-Raphson method which relies on the second-order Taylor's expansion approximation of the function $f(\sigma)$. Specifically, the Newton's method approximates

$$f(\sigma + p) \approx f(\sigma) + \nabla f(\sigma)^T p + \frac{1}{2} p^T \nabla^2 f(\sigma) p, \tag{7}$$

where the gradient and the Hessian of $f(\sigma)$ are given respectively by

$$\nabla f(\sigma) = J(\sigma)^T (F(\sigma) - V_m), \tag{8}$$

and

$$\nabla^2 f(\sigma) = J(\sigma)^T J(\sigma) + \sum_k r_k(\sigma) \nabla^2 r_k(\sigma), \tag{9}$$

with $J(\sigma)$ the Jacobian matrix of $r(\sigma) := F(\sigma) - V_m$.
The search direction p is computed by imposing optimality condition for p to EITNL with $f(\sigma)$ approximated as in (7):

$$\frac{\partial f(\sigma + p)}{\partial p} = \nabla f(\sigma)^T + \nabla^2 f(\sigma) p = 0, \tag{10}$$

which implies that

$$\nabla^2 f(\sigma) p^N = -\nabla f(\sigma). \tag{Newton-Raphson}$$

We can essentially approximate the Hessian matrix by ignoring all the second order terms from $\nabla^2 f(\sigma)$ in (9), so the search direction p in (Newton-Raphson) reduces to the following linear system

$$J^T(\sigma) J(\sigma) p^{GN} = -J^T(\sigma)(F(\sigma) - V_m). \tag{Gauss-Newton}$$

Gauss-Newton method starts from an initial guess σ_0 and performs a line search along the direction p_k^{GN} to obtain the new iterate σ_{k+1} as

$$\sigma_{k+1} = \sigma_k + p_k^{GN}. \tag{11}$$

In (Gauss-Newton), V_m is the measurement vector, the coefficient matrix which involves the Jacobian matrix, is a linear operator, however, due to its compact nature, it has an unbounded (discontinuous) inverse. This causes the solution to be unstable against variations in the data, hence violating Hadamard's third criterion for well posedness. Therefore, applying the Gauss-Newton method to problem (EITNL) yields inaccurate solutions; one could instead employ some form of regularization on the sought solution σ. The regularized Gauss-Newton

(RGN) method, using a generalized Tikhonov regularizer, consists in applying GN to the minimization problem:

$$\sigma^* = \arg\min_{\sigma} \{\mathcal{J}(\sigma;\lambda) = f(\sigma) + \lambda g(\sigma)\}, \quad g(\sigma) = \|L\sigma\|_2^2, \tag{12}$$

where $L \in \mathbb{R}^{n_T \times n_T}$ is a matrix representing a discrete differential operator.

The gradient and the approximated Hessian matrix of the objective function in (12) are respectively:

$$\nabla\mathcal{J}(\sigma;\lambda) = J(\sigma)^T(F(\sigma) - V_m) + \lambda L^T L\sigma, \tag{13}$$

$$\nabla^2\mathcal{J}(\sigma;\lambda) = \nabla^2 F(\sigma)(F(\sigma) - V_m) + J(\sigma)^T J(\sigma) + \lambda L^T L.$$

The search direction p_k from the current iterate satisfies the linear system

$$(J(\sigma_k)^T J(\sigma_k) + \lambda L^T L)p_k^{GN} = J(\sigma_k)^T(V_m - F(\sigma_k)). \tag{14}$$

An efficient minimization of the nonlinear Tikhonov regularized functional (12) is proposed in [16] for small or medium-scale problems, by exploiting the singular value decomposition of the Jacobian matrix J.

In our implementation of the RGN method we consider L to be the second order high-pass filter (Laplace prior) with homogeneous Neumann boundary conditions. Due to the triangular discretization of the domain Ω, each row of the graph Laplacian L has only 4 non-zero elements: it has value -1 for each adjacent triangle, and 3 for the triangle itself.

4 EITNL with Non-linear/Linear Regularization Term

In this section, we present a non-linear reconstruction framework represented by the following NLLS optimization problem

$$\sigma^* = \arg\min_{\sigma} \left\{ \mathcal{J}(\sigma;\lambda) = \frac{1}{2}\|F(\sigma) - V_m\|_2^2 + \lambda R(\sigma) \right\}, \tag{15}$$

where the regularizer term $R(\sigma)$ can assume one of the following forms

(a) $R_{NL}(\sigma) = \phi(\|D\sigma\|_2; a)$;
(b) $R_L(\sigma) = \|L\sigma\|_2^2$.

In (a), $D \in \mathbb{R}^{n_E \times n_T}$ is a matrix representing the discrete gradient operator which vanishes to zero everywhere but the mesh edges, and is defined as follows

$$D_{ij} = \begin{cases} 1 \text{ if } \tau_j \bigcap \tau_k = e_i\,,\ j < k\,,\ k \neq j\,,\ k = 1,\ldots,n_T, \\ -1 \text{ if } \tau_j \bigcap \tau_k = e_i\,,\ j > k\,,\ k \neq j\,,\ k = 1,\ldots,n_T, \\ 0 \text{ otherwise}\,, \end{cases} \tag{16}$$

where the two nonzero entries per row correspond to position of adjacent triangles τ_j, τ_k sharing the edge e_i. Applying homogeneous Neumann boundary

conditions, $\nabla\sigma|_{\partial\Omega} = 0$, the rows of D corresponding to the boundary edges can be eliminated from D, thus, n_E will refer to the number of inner mesh edges.

The function $\phi : \mathbb{R} \to \mathbb{R}^+$ in (a) is a numerically tractable version of the ℓ_0 pseudo-norm promoting sparsity and depending on a parameter a. Among the non-convex sparsity-promoting regularizers characterized by tunable degree of non-convexity, we consider in the proposed FB framework the Minimax Concave Penalty, introduced in [18], which reads as:

$$\phi(t;a) = \begin{cases} -\frac{a}{2}t^2 + \sqrt{2a}t & \text{if } |t| < \sqrt{\frac{2}{a}}, \\ 1 & \text{if } |t| \geq \sqrt{\frac{2}{a}}, \end{cases} \tag{17}$$

where $a > 0$ modulates the concavity of the regularizer.

The non-convex optimization problem (15) is smooth for R_L and non-smooth for R_{NL}.

Motivated by the following result on a generic point $\sigma^{(n+1)}$ of an iterative scheme, the minimization of $\mathcal{J}(\sigma;\lambda)$ in (15) will be carried out by a Forward-Backward (FB) splitting scheme, introduced in [7].

Proposition 2: Let F be a Frechét differentiable operator defined in (2), then

$$\sigma^{(n+1)} \in \text{prox}_{\gamma g}\left(\sigma^{(n)} - \gamma J^T(\sigma^{(n)})(F(\sigma^{(n)}) - V_m)\right) \tag{18}$$

is equivalent to

$$\sigma^{(n+1)} \in \arg\min_{\sigma}\left\{\tilde{f}(\sigma) + g(\sigma)\right\}, \tag{19}$$

where $\tilde{f}(\sigma) = \frac{1}{2}\|F(\sigma^{(n)}) - V_m + J(\sigma^{(n)})(\sigma - \sigma^{(n)})\|_2^2$, and $g(\sigma) = \lambda R(\sigma)$.

Proof: Consider the minimization problem

$$\sigma^* \in \arg\min_{\sigma}\left\{\tilde{f}(\sigma) + g(\sigma)\right\}. \tag{20}$$

The first order necessary conditions for (20), satisfied for σ^*, read as

$$0 \in \partial\tilde{f}(\sigma^*) + \partial g(\sigma^*), \tag{21}$$

where ∂ denotes the subdifferential, and

$$\partial\tilde{f}(\sigma) = J^T(\sigma^{(n)})\left(F(\sigma^{(n)}) - V_m + J(\sigma^{(n)})(\sigma - \sigma^{(n)})\right). \tag{22}$$

For any fixed $\gamma > 0$ the followings are equivalent:

$$0 \in \gamma\partial\tilde{f}(\sigma^*) + \gamma\partial g(\sigma^*) \tag{23}$$

$$0 \in \gamma\partial\tilde{f}(\sigma^*) - \sigma^* + \sigma^* + \gamma\partial g(\sigma^*) \tag{24}$$

$$(I + \gamma\partial g)(\sigma^*) \in (I - \gamma\partial\tilde{f})(\sigma^*) \tag{25}$$

$$\sigma^* \in (I + \gamma \partial g)^{-1}(I - \gamma \partial \tilde{f})(\sigma^*). \tag{26}$$

Equation (26) can be interpreted as fixed point scheme that generates a sequence $\{\sigma^{(n)}\}$ by iterating:

$$\sigma^{(n+1)} \in (I + \gamma \partial g)^{-1}(I - \gamma \partial \tilde{f})(\sigma^{(n)})$$

$$\sigma^{(n+1)} \in (I + \gamma \partial g)^{-1}\left(\sigma^{(n)} - \gamma J^T(\sigma^{(n)})(F(\sigma^{(n)}) - V_m)\right)$$

which can be rewritten as the proximal map (18). ■

Considering that the proximal map (18) can be rewritten as

$$\begin{aligned}\sigma^{(n+1)} \in \arg\min_{\sigma} \{ & g(\sigma) \\ & + \tfrac{1}{2\gamma}\|\sigma - (\sigma^{(n)} - \gamma J^T(\sigma^{(n)})(F(\sigma^{(n)}) - V_m))\|_2^2 \Big\},\end{aligned} \tag{27}$$

and that $F(\sigma^{(n)}) - V_m + J(\sigma^{(n)})(\sigma - \sigma^{(n)})$ represents a good linear approximation model of problem (15), then we can apply a first order optimization method to solve the problem. In particular, given $\sigma^{(0)}$, $\gamma > 0$, $\lambda > 0$, we apply the Forward-Backward scheme which iterates for $n = 1, \ldots$ as follows:

Forward Step
$z^{(n)} = \sigma^{(n)} - \gamma J^T(\sigma^{(n)})(F(\sigma^{(n)}) - V_m)$
Backward Step
$\sigma^{(n+1)} \in \arg\min_{\sigma} \left\{ \frac{1}{2\gamma} \left\|\sigma - z^{(n)}\right\|_2^2 + \lambda R(\sigma) \right\}.$

The FB scheme is stopped as soon as the relative residual is less than a given tolerance.

4.1 Using a Linear Regularizer R_L

In this case the Backward step in the FB algorithm is defined as follows

$$\sigma^{(n+1)} \leftarrow \arg\min_{\sigma} \left\{ \frac{1}{2} \left\|\sigma - z^{(n)}\right\|_2^2 + \gamma\lambda \|L\sigma\|_2^2 \right\} \tag{28}$$

with L being the Laplace prior. Being (28) a convex and differentiable minimization problem, an approximate solution $\sigma^{(n+1)}$ is explicitly given by solving the linear system

$$\left(I + \frac{\gamma\lambda}{2} L^T L\right) \sigma = z^{(n)}. \tag{29}$$

The system matrix is symmetric, positive definite, but unstructured, therefore the linear system (29) admits a unique solution obtained very efficiently by a few iterations of a warm-started iterative solver.

4.2 Using a Non-linear Regularizer R_{NL}

The backward step using $\phi(\cdot; a)$ in (17) leads to a nonconvex-nonsmooth optimization problem. Nevertheless, thanks to the properties of the penalty function, we can apply the so called Convex-Non-Convex strategy [1],[15], to ensure the convexity of the overall functional. The convexity conditions are summarized in the following Proposition.

Proposition 3: Let $R_{NL} = \phi(x; a)$, with $\phi(x; a)$ defined in (17), then the sufficient convexity condition for the functional in the Backward step of the FB algorithm is defined as

$$a < \frac{1}{\gamma\, \lambda\, e_{MAX}}\,, \tag{30}$$

where e_{MAX} is the maximum eigenvalue of matrix $D^T D \in \mathbb{R}^{n_T \times n_T}$.

The proof follows from [8].

By introducing the auxiliary variable $t \in \mathbb{R}^{n_E}$, the Backward Step can be rewritten in the following equivalent form

$$\begin{aligned} \{\sigma^*, t^*\} \leftarrow \arg\min_{\sigma,t} \Big\{ & \tfrac{1}{2\gamma} \left\|\sigma - z^{(n)}\right\|_2^2 \\ & + \lambda \textstyle\sum_{j=1}^{n_E} \left[\phi\left(|t_j|\,; a\right)\right] \Big\} \\ \text{subject to :} \quad & t = D\sigma. \end{aligned} \tag{31}$$

To solve the constrained optimization problem we introduce the augmented Lagrangian functional

$$\begin{aligned} \mathcal{L}(\sigma, t; \rho; \lambda, a) = & \frac{1}{2\gamma} \left\|\sigma - z^{(n)}\right\|_2^2 + \lambda \sum_{j=1}^{n_E} \phi\left(|t_j|\,; a\right) \\ & - \langle \rho, t - D\sigma \rangle + \frac{\beta}{2} \|t - D\sigma\|_2^2 \end{aligned}$$

where $\beta > 0$ is a scalar penalty parameter and $\rho \in \mathbb{R}^{n_E}$ is the vector of Lagrange multipliers associated with the linear constraint $t = D\sigma$. The following saddle-point problem is then considered:

$$\begin{aligned} \text{Find} \quad & (\sigma^*, t^*; \rho^*) \in \mathbb{R}^{n_T} \times \mathbb{R}^{n_E} \times \mathbb{R}^{n_E} \\ \text{s.t.} \quad & \mathcal{L}\left(\sigma^*, t^*; \rho; \lambda, a\right) \leq \mathcal{L}\left(\sigma^*, t^*; \rho^*; \lambda, a\right) \\ & \leq \mathcal{L}\left(\sigma, t; \rho^*; \lambda, a\right) \\ & \forall (\sigma, t; \rho) \in \mathbb{R}^{n_T} \times \mathbb{R}^{n_E} \times \mathbb{R}^{n_E} \end{aligned}$$

Given vectors $\sigma^{(k)}$ and $\rho^{(k)}$ computed at the kth iteration (or initialized if $k = 0$), the $(k+1)$th iteration of the ADMM-based iterative scheme applied to the solution of the saddle-point problem is split into the following three sub-problems:

$$\begin{aligned} t^{(k+1)} & \leftarrow \arg\min_{t \in \mathbb{R}^{n_E}} \mathcal{L}\left(\sigma^{(k)}, t; \rho^{(k)}; \lambda, a\right) \\ \sigma^{(k+1)} & \leftarrow \arg\min_{\sigma \in \mathbb{R}^{n_T}} \mathcal{L}\left(\sigma, t^{(k+1)}; \rho^{(k)}; \lambda, a\right) \\ \rho^{(k+1)} & \leftarrow \rho^{(k)} - \beta\left(t^{(k+1)} - D\sigma^{(k+1)}\right). \end{aligned}$$

The minimization sub-problem for σ can be rewritten as follows:

$$\sigma^{(k+1)} \leftarrow \arg\min_{\sigma \in \mathbb{R}^{n_T}} \left\{ \frac{1}{2\gamma} \left\| \sigma - z^{(n)} \right\|_2^2 + \left\langle \rho^{(k)}, D\sigma \right\rangle + \frac{\beta}{2} \left\| t^{(k+1)} - D\sigma \right\|_2^2 \right\}.$$

The first-order optimality conditions of the quadratic minimization problem lead to the following linear system:

$$\left(\frac{1}{\gamma} I + \beta D^T D \right) \sigma = \frac{1}{\gamma} z^{(n)} + \beta D^T \left(t^{(k+1)} - \frac{1}{\beta} \rho^{(k)} \right).$$

Since $\gamma, \beta > 0$, the system matrix is symmetric, positive definite. However, D represents the discretization of first order derivatives on a unstructured 2D mesh, thus matrix $D^T D$ is unstructured, and the linear system cannot benefit of fast transform solvers. The unique solution of the linear system can be efficiently obtained via a few steps of warm-started iterative solver.

Solving the Sub-problem for t. Recalling the separability property of $\phi(\cdot; a)$, defined in (17), the minimization sub-problem for t can be rewritten in the following element-wise (edge-per-edge) form:

$$t^{(k+1)} \leftarrow \arg\min_{t \in \mathbb{R}^{n_E}} \sum_{j=1}^{n_E} \left\{ \lambda \phi(|t_j|; a) - \rho_j^{(k)} t_j + \frac{\beta}{2} \left(t_j - (D\sigma^{(k)})_j \right)^2 \right\}, \tag{32}$$

where constant terms have been omitted. Therefore, solving (32) is equivalent to solving n_E one-dimensional problems for t_j, $j = 1, \ldots, n_E$

$$t_j^{(k+1)} \leftarrow \arg\min_{t \in \mathbb{R}} \left\{ \lambda \phi(|t|; a) - \rho_j^{(k)} t + \frac{\beta}{2} \left(t - (D\sigma^{(k)})_j \right)^2 \right\}. \tag{33}$$

After some algebraic manipulation, we can rewrite (33) in the following form

$$t_j^{(k+1)} \leftarrow \arg\min_{t \in \mathbb{R}} \left\{ \frac{\alpha}{2} \left(t - r_j^{(k+1)} \right)^2 + \phi(|t|; a) \right\}, \tag{34}$$

where

$$\alpha := \frac{\beta}{\lambda}, \qquad r_j^{(k+1)} := (D\sigma^{(k)})_j + \frac{1}{\beta} \rho_j^{(k)}. \tag{35}$$

Based on results in [[8], Prop.7.1], we can ensure strong convexity of the subproblems for the primal variables t_j, $j = 1, \ldots, n_E$, if and only if the following condition holds:

$$\alpha > a \;\Leftrightarrow \beta > a\,\lambda\,. \tag{36}$$

In case that (36) is satisfied, following [[8], Prop.7.1], the unique solutions of the strongly convex problems in (34) can be obtained in closed-form by applying the soft-thresholding operator:

$$t_j^{(k+1)} = \min\left\{\max\left\{\nu - \zeta/|r_j^{(k+1)}|\,,\,0\right\}\,,\,1\right\} r_j^{(k+1)}, \tag{37}$$

where $\nu = \frac{\alpha}{\alpha - a}$, and $\zeta = \frac{\sqrt{2a}}{\alpha - a}$.

5 Numerical Experiments

In this section we evaluate the proposed method on a set of synthetic 2D experiments. All examples but the last one, labeled as "heart and lungs", simulate a circular tank slice of unitary radius with a boundary ring of 16 electrodes; drive current value is set to $0.1\,mA$ and conductivity of the background liquid is set to $\sigma_0 = 0.02\,\Omega m^{-1}$. Measurements are simulated through *opposite injection - adjacent measurement* protocol via EIDORS software using a generic forward mesh of $n_T = 39488$ triangles and $n_V = 19937$ vertices. A coarse backward mesh was employed for inverse EIT solutions, with $n_T = 5056$ triangles without overlapping elements with the ones of the fine forward mesh so that to avoid the so called *inverse crimes* in EIT [3].

The performance is assessed both qualitatively and quantitatively. The quantitative analysis is performed via the following *slice metric*:

$$\epsilon_s = \frac{\|\sigma_{GT} - \sigma^*\|_2^2}{\|\sigma_{GT}\|_2^2}\,, \tag{38}$$

which measures how well the original conductivity distribution is reconstructed in case a ground truth conductivity distribution σ_{GT} is known. In order to allow for a mesh independent comparison, the conductivity distributions are evaluated on an image structure of dimension 576×576 pixels. In all the experiments and for all the algorithms, we hand-tuned their regularization parameter so as to achieve the lowest possible ϵ_s norm error.

In the last example we applied our framework to a more realistic dataset "heart and lungs" where the measurements are given in 2D circular tank with chest shaped conductivity targets in calibrated phantom at Rensselaer Polytechnic with ACT 3 EIT system, and kindly provided in [10]. This data have been measured with trigonometric injection current pattern over a boundary ring of 32 Electrodes. The tank width is $30\,cm$ in diameter; the electrodes are 2.5 cm long and $1.6\,cm$ tall. The saline conductivity was $424\,mS/m$. The agar targets of the "lungs" had a conductivity of $240\,mS/m$, and the "heart" was $750\,mS/m$. The experimental setting is illustrated in Fig. 6 (first column), thus imposing a piecewise-constant conductivity distribution. Since the conductivity distribution was assumed to be piecewise constant, the FB framework involved the R_{NL} non-linear regularizer, setting the parameter a accordingly to obtain a convex backward step.

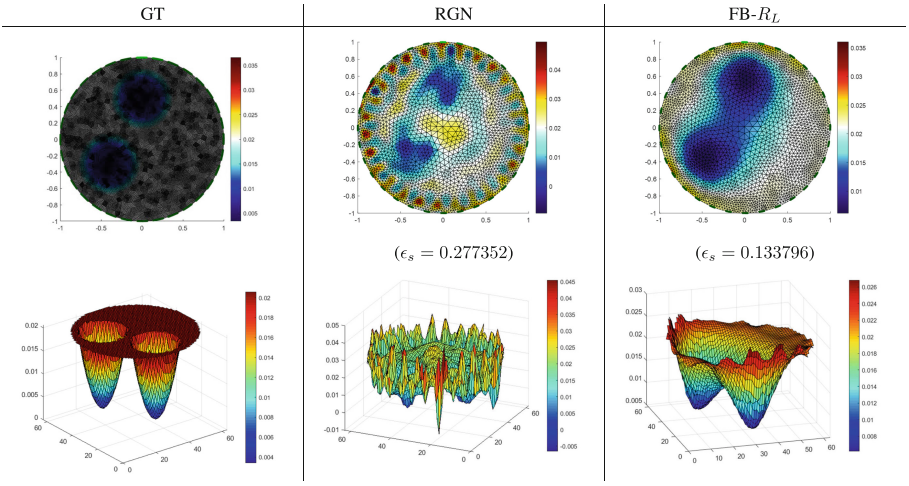

Fig. 1. Reconstructions using smooth R_L regularizer: GT (first column), RGN (second column), our (third column).

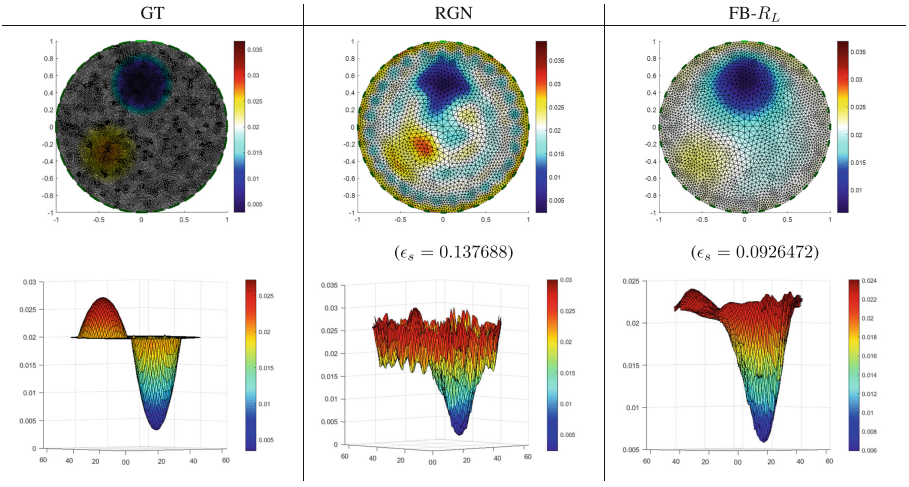

Fig. 2. Reconstructions using smooth R_L regularizer: GT (first column), RGN (second column), our (third column).

In all the examples we compared the Regularized Gauss Newton method (RGN) using Laplace prior with the proposed FB-R_L, or FB-R_{NL} algorithms. The regularization parameters λ for all the experiments have been chosen by trial and error to produce the best reconstructions in terms of ϵ_s. The setup is blind, that is no a priori information about the dimensions or locations of the inclusions is considered, only the kind of conductivity distribution is preliminary given such as *smooth* or *piecewise constant*. This simple a priori knowledge about

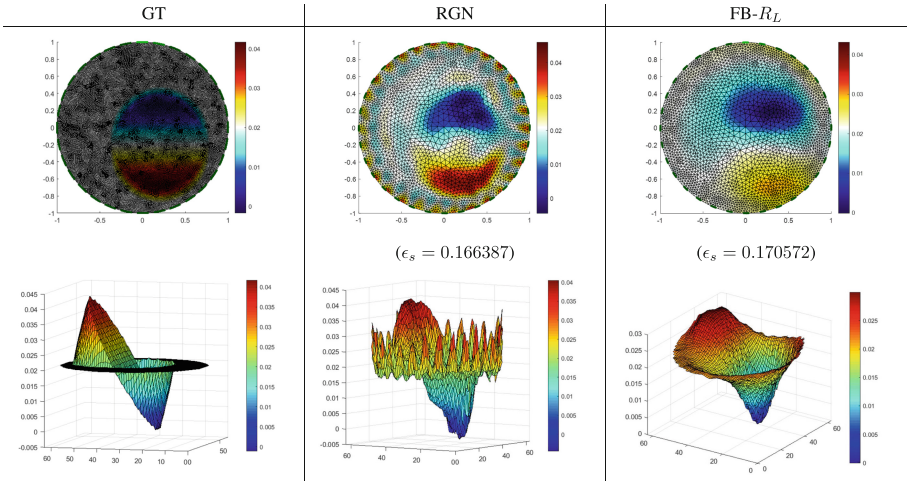

Fig. 3. Reconstructions using smooth R_L regularizer: GT (first column), RGN (second column), our (third column).

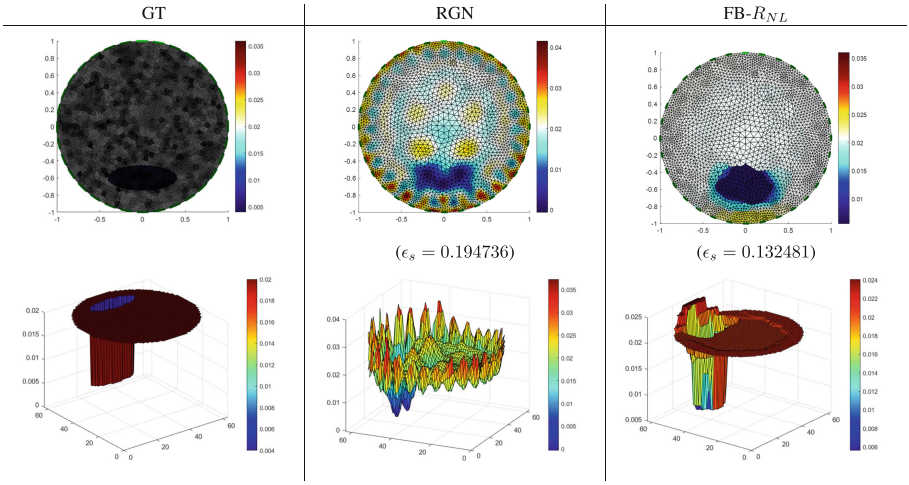

Fig. 4. Reconstructions using non-smooth R_{NL} regularizer: GT (first column), RGN (second column), our (third column).

the feature of the inclusions is used to select the regularizer $R(\sigma)$ in (15) as R_L or R_{NL}, respectively.

First, we compared the results obtained by RGN and FB-R_L algorithms when applied to the reconstruction of conductivity distribution characterized by smooth inclusions. The ground truth conductivity distributions are illustrated in Fig. 1, Fig. 2, Fig. 3 (first columns), and the reconstructed conductivities with RGN and FB-R_L are reported in Fig. 1, Fig. 2, Fig. 3 middle and right columns

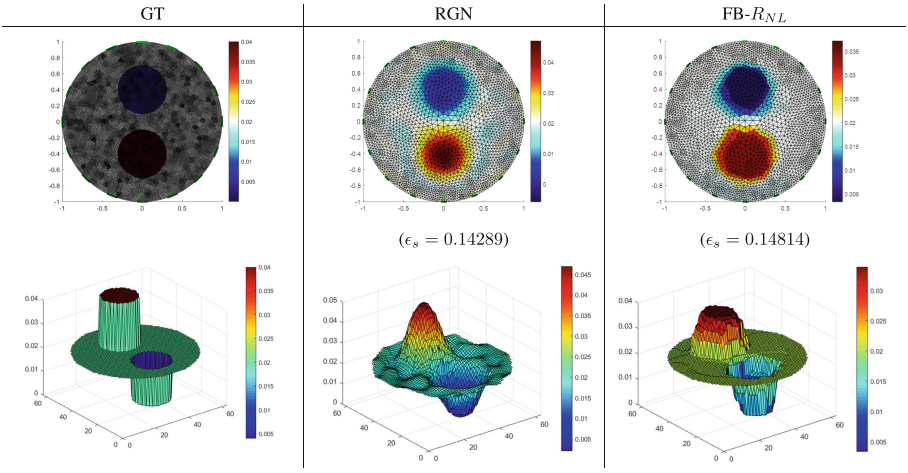

Fig. 5. Reconstructions using non-smooth R_{NL} regularizer: GT (first column), RGN (second column), our (third column).

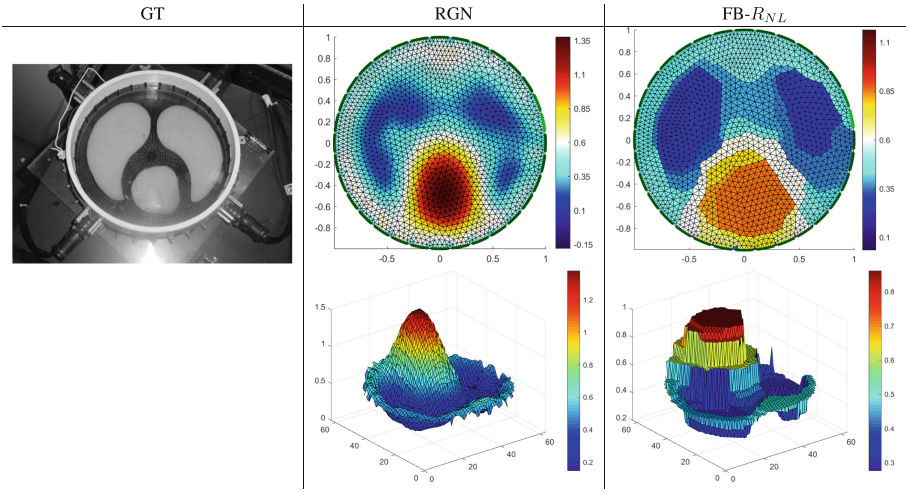

Fig. 6. Reconstructions of the "heart and lungs" example, using non-smooth R_{NL} regularizer: GT (first column), RGN (second column), our (third column).

respectively. Our approach provides always more stable results, which produce better reconstructions. The ϵ_s errors reported in the figures for each reconstruction confirm the improved accuracy of the proposed approach (Fig. 4).

In case the a priori knowledge of the conductivity distribution indicates that the sought anomalies are characterized by piecewise constant shape, the framework FB-R_{NL} is the most suitable to use. In the examples illustrated in Fig. 5, Fig. 6 we compare the reconstruction results obtained by the RGN algorithm

with the proposed FB-R_{NL} method, reported in Fig. 5, Fig. 6 middle and right columns, respectively. From a visual inspection we observe that our proposal better preserve the piecewise constant shape of the anomalies with respect to the round-shaped results provided by RGN.

6 Conclusions

In this paper we proposed a FB iterative solution to the inverse nonlinear EIT problem. This allowed to treat the non-linearity of the EIT model and thus to obtain more accurate conductivity distributions. Moreover, according to the prior knowledge on the sought conductivities, the proposed framework can easily integrate a smooth regularizer as well as a sparsity-inducing penalty to enforce the reconstruction of piecewise constant conductivity distributions. Future work will address the theoretical analysis on the convergence of the FB framework, and will further investigate the use of other numerical regularization methods for nonlinear inverse problems to deal with the challenging nonlinear EIT problem.

Acknowledgment. This work was supported in part by the National Group for Scientific Computation (GNCS-INDAM), Research Projects 2020, and in part by MIUR RFO projects.

References

1. Blake, A., Zisserman, A.: Visual Reconstruction. Cambridge MIT Press, Cambridge (1987)
2. Borsic, A.: Regularisation methods for imaging from electrical measurements, Ph.D. thesis, School of Engineering, Oxford Brookes University, UK (2002)
3. Borsic, A., Graham, B.M., Adler, A., Lionheart, W.R.B.: In Vivo impedance imaging with total variation regularization. IEEE Trans. Med. Imaging **29**(1), 44–54 (2010)
4. Calderón, A.P.: On an inverse boundary value problem. In: Seminar on Numerical Analysis and its Applications to Continuum Physics, pp. 65–73 (1980)
5. Cheng, K.-S., Isaacson, D., Newell, J.C., Gisser, D.G.: Electrode models for electric current computed tomography. IEEE Trans. Biomed. Eng. **36**(9), 918–924 (1989)
6. Cheney, M., Isaacson, D., Newell, J., Simske, S., Goble, J.: NOSER: an algorithm for solving the inverse conductivity problem. Int. J. Imaging Syst. Technol. **2**, 66–75 (1990)
7. Combettes, P.L., Wajs, V.R.: Signal recovery by proximal forward-backward splitting. Multiscale Model. Simul. **4**, 1168–1200 (2005)
8. Huska, M., Lanza, A., Morigi, S., Selesnick, I.: A convex non-convex variational method for the additive decomposition of functions on surfaces. Inverse Prob. **35**(12), 124008–124041 (2019)
9. Huska, M., Lazzaro, D., Morigi, S., Samorè, A., Scrivanti, G.: Spatially-adaptive variational reconstructions for linear inverse electrical impedance tomography. J. Sci. Comput. **84**(3), 1–29 (2020). https://doi.org/10.1007/s10915-020-01295-w
10. Isaacson, D., Mueller, J.L., Newell, J.C., Siltanen, S.: Reconstructions of chest phantoms by the d-bar method for electrical impedance tomography. IEEE Trans. Med. Imaging **23**(7), 821–828 (2004)

11. Jauhiainen, J., Kuusela, P., Seppanen, A., Valkonen, T.: Relaxed gauss-newton methods with applications to electrical impedance tomography. SIAM J. Imaging Sci. **13**(3), 1415–1445 (2020)
12. Lionheart, W.: EIT reconstruction algorithms: pitfalls, challenges and recent developments. Physiol. Meas. **25**(1), 125 (2004)
13. Liu, D., Kolehmainen, V., Siltanen, S., Seppänen, A.: A nonlinear approach to difference imaging in EIT; assessment of the robustness in the presence of modelling errors. Inverse Prob. **31**(3), 035012:1-035012:25 (2015)
14. Lechleiter, A., Rieder, A.: Newton regularizations for impedance tomography: convergence by local injectivity. Inverse Prob. **24**(6), 065009065009 (2008)
15. Nikolova, M.: Estimation of binary images by minimizing convex criteria. In: Proceedings of the IEEE International Conference on Image Processing, vol. 2, p. 108 (1988)
16. Pes, F., Rodriguez, G.: The minimal-norm Gauss-Newton method and some of its regularized variants. Electron. Trans. Numer. Anal. **53**, 459–480 (2020)
17. Vauhkonen, M., Vadasz, D., Karjalainen, P.A., Somersalo, E., Kaipio, J.P.: Tikhonov regularization and prior information in electrical impedance tomography. IEEE Trans. Med. Imaging **17**(2), 285–293 (1998)
18. Zhang, C.-H.: Nearly unbiased variable selection under minimax concave penalty. Ann. Stat. **38**(2), 894–942 (2010)